UNIVERSITAT DE BARCELONA

FACULTAT DE FÍSICA

Biophysics Master

A Lattice-Boltzmann simulation of a bead-polymer complex

Final Project 2008/09:
Carles Panadès i Guinart

Tutor: Dr. Ignasi Pagonabarraga Mora

Keywords: Lattice-Boltzmann, Molecular Dynamics, Fluid Dynamics, Polymer Physics

Contents

Abstract

A complex composed of a polymer and a colloid coupled together and immersed in a fluid, is simulated by means of the Lattice-Boltzmann Method and Molecular Dynamics. The system dynamics is characterized using dimensionless numbers.

Unravelling the properties of the complex might have severe implications in single molecule experiments or in any system similar to a polymer attached to rigid object, such as some molecular machines or the novel polymer-protein hybrid materials. In addition, the adhesion of the colloid to one of the edges of the polymer creates a unique frame for the latter in the sense that many new properties may arise due to the shear effects induced near the colloid and the symmetry breaking that its presence represents for the polymer.

1 Introduction

1.1 Motivation

Single Molecule Experiments (SME) have become of great importance in the field of Biophysics mainly because these techniques allow physicists to monitorize and manipulate individual molecules [1]. Some representative examples are Atomic Force Microscopy (AFM), Laser Optical Tweezers (LOTs), and Magnetic Tweezers (MTs). Of course, the choice of a technique in particular depends strongly on the experiment requirements, such as the force range or the space resolution. From the biophysical point of view, understanding the dynamics of biomolecules, such as biopolymers and proteins, is a crucial matter.

However, in most experiments involving biomolecules, the object under study is not only a single molecule but an aggregate composed of at least two different objects, whose interaction may be neglected in some cases. In order to analyze a possible coupling, the present work is focused on simulating a bead-polymer complex immersed in a fluid using the Lattice-Boltzmann Method (LBM) for the fluid and the colloid, and Molecular Dynamics (MD) for the evolution of the polymer.

A practical application might be related with the improvement of the LOTs calibration. This technique uses an optical gradient force created by a focused laser beam that interacts with an object, which possesses an index of refraction higher than the one of the surrounding medium. This gradient can be used to trap a great variety of objects of different sizes: microbeads, eukaryotic cells, bacteria, viruses, etc.

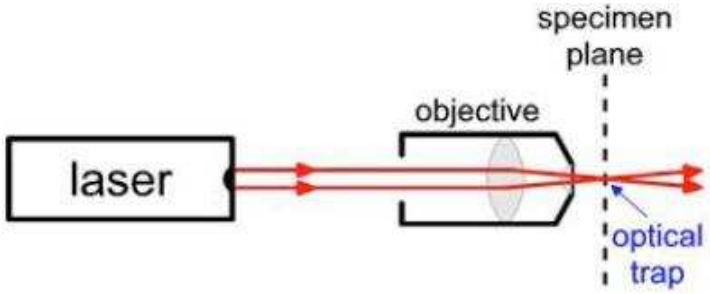

Figure 1: Typical experimental set-up of LOTs.

The typical experimental set-up consists on a laser (usually near infrared) that is collimated by a high numerical aperture lens (Figure 1). For practical purposes, let us focus in the case of a trapped microbead. This object is a sphere made of polystyrene or silica, and remains still in the focus of the laser. The ends of the molecules under study are labelled with different molecules, like biotin and digoxigenin, in an attempt to avoid double attachments between the two ends of a single molecule and the same

bead. In a very good approximation the trapping potential can be considered harmonic, yielding to a force proportional to the distance between the particle and the center of the trap, $F = -kr$. In this expression, k represents the stiffness of the trap and has to be determined via in the calibration process. The bead is assumed to behave as a Brownian particle trapped in a harmonic potential [1]. Thus, the Langevin equation that describes its dynamics should be:

$$m\ddot{x}(t) = -\gamma\dot{x}(t) - kx(t) + f_R(t) \tag{1}$$

where m is the mass of the particle, γ is the drag coefficient, and $f_R(t)$ is the stochastic force experienced by the particle due to the thermal motion of the molecules [2]. The latter is assumed to behave as white noise:

$$\left\langle f_R(t) f_R(t') \right\rangle = 2k_b T\gamma\delta(t - t') \tag{2}$$

Since the microbead is spherical and moves in a low Reynolds number regime, it follows the Stokes' law in a very good approximation:

$$\gamma = 6\pi\eta R \tag{3}$$

where η is the medium's dynamic viscosity, and R the radius of the particle. Neglecting inertial terms (the system is overdamped due to the viscosity), the former expression is reduced to:

$$f_R(t) = \gamma\dot{x}(t) + kx(t) \tag{4}$$

By taking the Fourier transform and the modulus squared, it is obtained the analytical expression of the power spectrum:

$$S(f) = |x(f)|^2 = \frac{k_B T}{\gamma\pi^2 \left(f^2 + f_c^2\right)} \tag{5}$$

where $f_c^2 = k/2\pi\gamma$ is the corner frequency and can be found easily after a fitting with the experiment. This magnitude is measured *in situ*, then the LOTs are calibrated instantanously. Clearly, the drag force depends on the radius of the bead. This statement is quite correct when the length scale of the polymer is small in comparison with the bead radius. However, as the polymer extends [3], its size becomes larger and somehow the Stokes' law should take into account some kind of effect. Therefore, changes on the drag coefficient of the complex bead-biopolymer ought to be considered for extended polymers and the experimental results might be biased somehow in this situation. Whether this effect can be relevant in the colloid dynamics or not, might be unravelled from our simulations.

Another potential implication is related with some experiments with polymers that undergo cyclic motions when are subjected to flow shears

[4]. A polymer is tethered to a static wall, while another wall moves with constant velocity, thus creating a constant Couette shear on the fluid. As a consequence, the chain performs a cyclic motion with a well-defined period. Somehow, our system shares great similarities with that system: the polymer is attached to a (moving) wall and relevant shear effects do occur near the colloid surface because of the relative movement between the colloid and the fluid. Hence, some characteristic time belonging to the colloid moving through the fluid, might make an appearance in the polymer dynamics.

Moreover, polymers are fascinating for theirselves. A knowledgeable reader on polymers may know that their related magnitudes feature a scaling law behaviour [5,6]. For instance, renormalization theory and numerical simulations show that the characteristic size scales with a critical exponent that depends on the model under consideration. Critical exponents are connected with some symmetries. In our concrete case, there is a clear symmetry breaking due to the colloid attachment on the chain edge. Thus, new properties on the polymer may arise because of the so-mentioned symmetry breaking.

Last but not least, our model might look rather simplistic, but will provide us with a first glimpse of how a biopolymer interacts with a more rigid object, like a bead or a protein. Currently, large efforts are being devoted to the development of new polymer-protein hybrid materials because of their unusual properties [7]. These hybrids have a large potential in the manufacture of sensors, nanomachine parts, and drug-delivery systems, since they combine the specific biological functions of proteins with the advantageous bulk and processing properties of polymers. Due to its applicability, their interaction with their surrounding media is a very pertinent question to be addressed. In addition, the adhesion of a polymer to other kind of proteins, like molecular machines, in the RNA transcription process or the intracellular transport is crucial topic of the state of the art in Biophysics [8].

As a natural consequence, in all cases understanding the effects of these coupling will provide us with better measurements and novel ways to access molecular information from this type of complexes for sure.

1.2 Project Outline

The present work is structured as follows. Firstly, Section 2 contains the methodology, including the details about the two simulation techniques and the definition of the dimensionless parameters that characterize the system under study. Then, Section 3 includes and explains all the relevant results. Finally, Section 4 is composed of some conclusive remarks as well as future directions of study.

2 Methodology

Essentially, the simulation method comprises two techniques. On the one hand, the Lattice-Boltzmann Method (LBM) is very appropriate to characterize a surrounding fluid with any imaginable boundary conditions [9] and has been used extensively in Biophysics [10,11]. Since a colloid can be interpreted as a special boundary inside the fluid, the LBM is also a proper technique to deal with these kind of objects [12]. On the other hand, Molecular Dynamics (MD) are used to simulate the polymer behaviour inside a fluctuating fluid. Some authors [13-16] have been successful to couple a polymer with a lattice-Boltzmann fluid but so far it has been never attempted to couple a polymer with a colloid immersed in a solvent.

In addition, the utilization of a dimensionless group will be of great assistance towards the characterization of the system [17].

2.1 Lattice-Boltzmann Method

The Lattice Boltzmann Method (LBM) is an advanced computational technique very helpful in the simulation of all kinds of fluids with complex boundaries. As its name indicates, these technique applies the Boltzmann equation at each node of a lattice that reticulates the whole space. The central quantity is the discretized one-particle velocity distribution function, $n_i(\mathbf{r}, t)$, which describes the density of particles with a discrete velocity $\mathbf{c}_i$, at point of the lattice located at $\mathbf{r}$, at a discrete time t. The hydrodynamic fields, mass density ρ, momentum density $\mathbf{j} = \rho\mathbf{c}_i$, and momentum flux $\mathbf{\Pi}$ are moments of that distribution:

$$\rho = \sum_i n_i \mathbf{c}_i \ , \mathbf{j} = \sum_i n_i \mathbf{c}_i \ , \mathbf{\Pi} = \sum_i n_i \mathbf{c}_i \mathbf{c}_i \tag{6}$$

The time evolution of $n_i(\mathbf{r}, t)$ is the Lattice-Boltzmann equation:

$$n_i(\mathbf{r} + \mathbf{c}_i \Delta t, t + \Delta t) = n_i(\mathbf{r}, t) + \Delta_i \left[\mathbf{n}(\mathbf{r}, t)\right] \tag{7}$$

where Δ_i is the change in n_i because of the instantaneous collisions at the lattice sites and Δt is the time step between collisions. A computational useful form for the collision operator can be constructed by linearizing about the local equilibrium:

$$\Delta_i(\mathbf{n}) = \Delta_i(\mathbf{n}^{eq}) + \sum_j L_{ij}(n_j - n_j^{eq}) \tag{8}$$

where L_{ij} is the linearized collision operator, and $\Delta_i(\mathbf{n}^{eq}) = 0$. It is remarkable that this equation is second-order accurate in space and time, so it can simulate all the Navier-Stokes phenomenology without imposing additional artifices.

Some of the previous parameters, such as Δ_i or $\mathbf{c}_i$, depend on the lattice type. All the feasible lattices can be comprised in the notation DnQm, meaning that the lattice possesses n dimensions and m discrete velocities. In our simulation, the used model is the D3Q19 which comprises stationary particles and 18 velocities corresponding to the [100] and [110] directions of a simple cubic lattice (Figure 2).

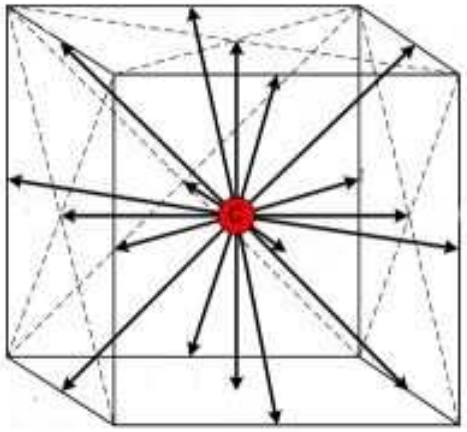

Figure 2: Representation of the D3Q19 model. While the arrows represent all the possible velocities, the red point is the stationary one.

Each velocity has a characteristic weight a_i^c that describes the fraction of particles with velocity $\mathbf{c}_i$ in a system at rest. Naturally, these weights must be normalized to one:

$$\sum_i a_i^c = 1 \tag{9}$$

The optimum choice of these coefficients is $a^0 = 1/3$, $a^1 = 1/18$, and $a^{\sqrt{2}} = 1/36$. Proceeding with the linearization, a suitable form for the equilibrium distribution is:

$$n_i^{eq} = a_i^c \left[\rho + \frac{\mathbf{j} \cdot \mathbf{c_i}}{c_s^2} + \frac{\rho \mathbf{uu} : \left(\mathbf{c}_i \mathbf{c}_i - c_s^2 \mathbf{1} \right)}{2 c_s^4} \right] \tag{10}$$

where $c_s^2 = 1/3$ represents the square of the lattice sound speed taking the value of the distance between nodes and the time step equal to one. Among all the hydrodynamic fields, the momentum flux is the only one modified in the collisional process.

However, force fields have not been considered so far, and should be included. The Lattice-Boltzmann equation that includes these external fields reads very similar to the former:

$$n_i(\mathbf{r} + \mathbf{c}_i \Delta t, t + \Delta t) = n_i(\mathbf{r}, t) + \Delta_i \left[\mathbf{n}(\mathbf{r}, t) \right] + f_i(\mathbf{r}, t) \tag{11}$$

where $f_i(\mathbf{r}, t)$ the additional force contribution to the lattice:

$$f_i = a_i^c \left[\frac{\mathbf{f} \cdot \mathbf{c_i}}{c_s^2} + \frac{(\mathbf{uf} + \mathbf{fu}) : \left(\mathbf{c}_i\mathbf{c}_i - c_s^2\mathbf{1}\right)}{2c_s^4} \right] \tag{12}$$

where $\mathbf{f}$ represents the force vector.

In order to simulate the hydrodynamics interactions between colloidal particles, the Lattice-Boltzmann scheme should be modified to incorporate these solid-fluid boundaries. Solid particles are defined by a boundary surface that cuts some of the links between the lattice nodes, so the moving fluid particles interact with the colloid. Therefore, a discrete representation of the particle surface is obtained and becomes preciser as the particle gets larger (Figure 3).

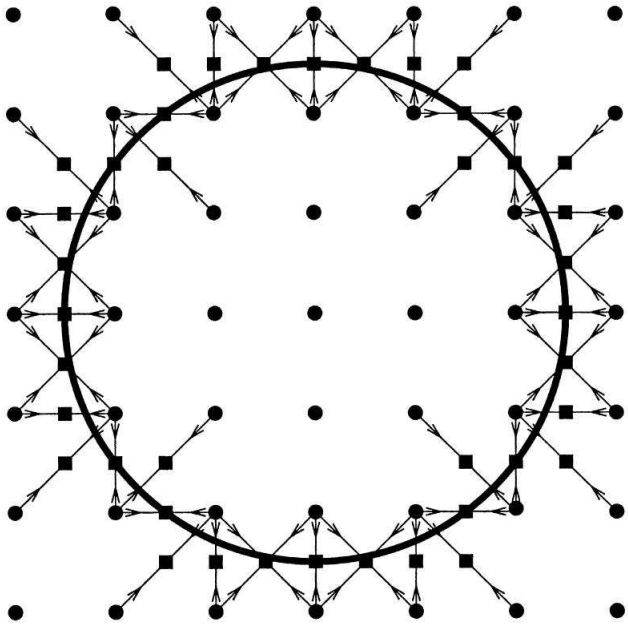

Figure 3: Definition of a colloid in a lattice: dots represent the lattice nodes while squares determine the colloid boundary.

Lattice nodes on either side of the boundary surface are treated identically. This simplifies the technical procedure while leaving the physics basically unaffected. Because of the relatively small volume inside each particle, the interior fluid quickly relaxes to a rigid-body movement. Generally, the most suitable place to locate the solid nodes is the midpoint of the lattice link. Consequently a semi-integer radius will be chosen for a colloid. In our case, if the solid site belongs to a particle p that moves at speed $\mathbf{U}_p$ and angular speed $\mathbf{\Omega}_p$, then its speed is:

$$\mathbf{u}_p = \mathbf{U}_p + \mathbf{\Omega}_p \times (\mathbf{r}_b - \mathbf{R}) \tag{13}$$

where $\mathbf{r}_b = \mathbf{r} - \frac{1}{2}\mathbf{c}_i$ is the location of the boundary node, and $\mathbf{R}$ is the coordinate of the center of center of mass. This speed sets the evolution of the populations that collide to the surface. As a result, a net momentum is transferred between the fluid and the solid site. By summing over all points belonging to the boundary, the total force and torque is computed.

In addition, our system need to be extended to simulate thermal fluctuations to simulate the brownian motion that would develop a colloidal particle. The best way of considering this phenomenon is by means of incorporating a random term into the momentum flux during the collisional process. Details of this inclusion and further simulation details can be found elsewhere [9].

2.2 Polymer-colloid coupling in the fluid

The former subsection contained all the relevant information concerning to the LBM and nothing has been commented about how to include the polymer. The polymer chain is modeled via a bead-spring model with an equilibrium bond length b between neighbouring beads. In order to prevent two consecutive beads from separating infinitely, a Finite Extendable Nonlinear Elastic (FENE) potential was chosen:

$$V_{\text{FENE}} = -\frac{1}{2}kR_0^2 \ln\left[1 - \left(\frac{r}{R_0}\right)^2\right] \tag{14}$$

where k is the stiffness of the nonlinear spring, and R_0 is the maximum monomer distance that is allowed by this FENE potential. The spring stiffness, $k = ak_bT/b^2$, was chosen so that the fluctuations in bond length, $\left\langle (r-b)^2 \right\rangle^{1/2} = b/\sqrt{a}$, were substantially smaller than the radius of gyration of the chain, R_g. In polymer physics, this magnitude is a very convenient way of expressing the size of the polymer because it can be directly measured in experiments and is defined as follows:

$$R_g^2 = \frac{1}{2N^2}\sum_{i=1}^{N}\sum_{j=1}^{N}(\mathbf{R}_i - \mathbf{R}_j)^2 \tag{15}$$

where N is the number of monomers and $\mathbf{R}_i$ is the position of the monomer number i. This magnitude is also equal to the square of the average distance between the segments and the center of mass of the polymer:

$$R_g^2 = \frac{1}{N}\sum_{i=1}^{N}(\mathbf{R}_i - \mathbf{R}_{\text{CM}})^2 \tag{16}$$

where $\mathbf{R}_{\text{CM}}$ represents the position of the center of mass:

$$\mathbf{R}_{\text{CM}} = \frac{1}{N}\sum_{j=1}^{N}\mathbf{R}_j \tag{17}$$

if all the monomers possess the same mass. Similarly, the velocity of the center of mass is just:

$$\mathbf{V}_{\mathrm{CM}} = \frac{1}{N}\sum_{j=1}^{N}\mathbf{V}_j \tag{18}$$

It can be demonstrated quite easily that:

$$R_g = \sqrt{\frac{N}{6}}b \tag{19}$$

for an entropically governed polymer chain. This expression is useful to set the inferior limit of R_g because for hydrodynamically governed polymers this magnitude will increase for sure. Therefore, considering $a = 30$ is more than in enough for our needs.

Continuing with the FENE potential, note that for small extensions it becomes the expression corresponding of the harmonic potential. For our practical purposes, the FENE force will be:

$$F_{\mathrm{FENE}} = -\frac{k(r-b)}{1-\left(\frac{r-b}{R_0}\right)^2} \tag{20}$$

because the equilibrium bond length, b, must be included. In the simulation, it is very important to keep $r - b < R_0$ because the force between beads would become repulsive and this situation has no physical sense. Hence, the maximum distance between monomers is $r_{\max} = R_0 + b$. In the great majority of our simulations, $R_0 = 4.0b$ is considered as a standard parameter.

In addition, in order to model the excluded volume effect and avoid the monomer overlapping, a hard-sphere [18] excluded volume interaction between the monomers was included, with a collision diameter $b/2$. Other excluded volume interactions, like a Lennard-Jones or a soft-sphere potential could be equally well used.

The equations of motion for the monomers are integrated using the Euler method [19]:

$$\mathbf{R}_i(t+dt) = \mathbf{R}_i(t) + \mathbf{V}_i dt + \frac{1}{2}\frac{\mathbf{F}_i}{m}dt^2 \tag{21}$$

$$\mathbf{V}_i(t+dt) = \mathbf{V}_i(t) + \frac{\mathbf{F}_i}{m}dt \tag{22}$$

where i refers to bead i and dt is the time step of the integrator, which is smaller than the lattice time step. Typically, $dt = 1/10, 1/100$ lattice time steps. Since the beads are immersed in a fluid, the force should also include the friction caused by the viscosity. This force is assumed to be proportional to the difference in velocity between the bead, $\mathbf{V}$, and the surrounding fluid, $\mathbf{u}(\mathbf{r})$:

$$\mathbf{F}_f = -\xi_0\left[\mathbf{V} - \mathbf{u}(\mathbf{r})\right] + \mathbf{F}_r \tag{23}$$

where ξ_0 is the bead viscosity coefficient and $\mathbf{F}_r$ is a random force introduced to balance the additional dissipation caused by not using no-slip boundary conditions on the bead surfaces. This force has a white noise behaviour:

$$\left\langle \mathbf{F}_r(t)\mathbf{F}_r(t')\right\rangle = 2k_bT\xi_0\delta(t-t') \tag{24}$$

The bead viscosity coefficient satisfies the Stokes' law with radius $b/4$. Since the monomers move continuously over the grid, while the velocity field is evaluated at the grid points, an interpolation procedure is used to evaluate $\mathbf{u}(\mathbf{r})$, employing the fluid velocities at the nodes of the cube that encloses the monomer. After calculating the weights of these grid points, w_i, the density, ρ_i, and the momentum density, $\rho_i\mathbf{u}_i$, the velocity field at the bead location is:

$$\mathbf{u}(\mathbf{r}) = \frac{\sum_i w_i\rho_i\mathbf{u}_i}{\sum_i w_i\rho_i} \tag{25}$$

where the sums are over all the eight nodes that form the interpolation cube. In order to conserve the total momentum, the force exerted by the monomer on the fluid is distributed to the surrounding nodes with the same weight function. Details of the polymer-fluid coupling can be found in the literature [13-16].

Let us turn now to the question of how the polymer and the colloid are coupled together. At some location on the surface of the colloid, there is a fictitious point called the base. Between the base and the monomer, the same interactions (FENE potential and hard-spheres) do occur with the difference that the force and the induced torque are applied to the update of the colloid. Last but not least, a hard-sphere interaction between the colloid and the monomers is taken into account with a collision radius equal to the sum of the colloid and the bead radii.

2.3 Dimensionless group

In fluid dynamics, the physicist is capable of discerning between different fluid regimes using dimensionless numbers. In general terms, our problem belongs to the same cathegory. Essentially, the colloid is advected or diffuses in the media and then the polymer chain will stretch in the streamwise direction or will change its configuration towards something similar to a random coil. Thus, the first step should be focused on characterizing the colloid. Basically, the colloid might have two trends: it can be advected or diffuse in the fluid. As a matter of fact, the Peclet number,

$$Pe = \frac{LV}{D} \tag{26}$$

relates the advection and the diffusion [20]. So, this dimensionless number should be appropriate to identify different regimes associated to the colloid.

In the previous expression, L is the length scale, V the characteristic velocity, and D the diffusion coefficient. Indeed, a suitable choice is $L \sim R$, $V \sim F/6\pi\eta R$, and $D = k_bT/\gamma$, where γ also comes from the Stokes' law. The Peclet number turns out to be:

$$Pe = \frac{FR}{k_bT} \tag{27}$$

For high Peclet numbers, the colloid experiences a net movement and drags the polymer, then stretching the polymer in this process. Thus for high Pe the colloid movement should govern the chain dynamics. However, in the contrary scenario (low Pe), both the colloid and the monomers should move randomly. Nevertheles, being in the advective regime (high Pe) may not be enough because the velocity of this net tranport can be as fast or slow as possible. The question is whether the advection is greater or smaller than the thermal noise. The quocient between the colloid velocity (Stokes' law):

$$V_c \sim \frac{F}{6\pi\eta R} \tag{28}$$

and the thermal agitation (equipartition theorem in the force direction):

$$V_f \sim \sqrt{\frac{k_bT}{m}} \tag{29}$$

where $m \sim \frac{4}{3}\pi R^3\rho$ is the colloid mass defines the advective ratio:

$$A \sim \frac{V_c}{V_f} \sim \frac{1}{3\sqrt{3\pi}}\frac{F}{\eta}\sqrt{\frac{R\rho}{k_bT}} \tag{30}$$

where ρ is the density and in all our simulations is set to the unity. Consider a high Peclet number. For $A \gg 1$, a strong advection is present, while for $A \ll 1$, the net tranport is very small and long times will be involved to see any advective effect.

In rheology, a complex fluid is usually characterized by means of a dimensionless number called the Weissenberg number, We. This number is defined as the ratio between the fluid and the polymer characteristic times [21]. The Zimm time is the relaxation time of the polymer:

$$t_Z \sim \frac{\eta R_g^3}{k_bT} \tag{31}$$

The Zimm time is obtained from the Zimm model, which assumes a polymer immersed in a fluid using a bead-spring model with hydrodynamic interactions. A major result from this model is $R_g \sim bN^\nu$, where ν is the polymer scaling factor that may depend on the model. For instance, considering the Zimm model in a bad and a good solvent gives $\nu \simeq 0.5$ and $\nu \simeq 0.6$, respectively. What is really important is the fact that the Zimm time goes

as the radius of gyration to the third power. For the fluid, there are two characteristic times: the viscous time and the time related with the shear induced by the colloid advection. The viscous time is defined:

$$t_V \sim \frac{R^2 \rho}{\eta} \tag{32}$$

whilst the other is the time that the colloid needs to travel the length scale of the problem:

$$t_S = \frac{L}{V} \sim \frac{6\pi\eta R^2}{F} \tag{33}$$

So, the Weissenberg number when the colloid diffuses would be:

$$We_1 \sim \frac{\eta^2 b^3 N^{3\nu}}{\rho k_b T R^2} \tag{34}$$

but in the advective regime:

$$We_2 \sim \frac{F b^3 N^{3\nu}}{k_b T R^2} \tag{35}$$

which can be expressed as a function of the Peclet number and the cubic term of the ratio between the radius of gyration and the colloid radius:

$$We_2 \sim Pe \frac{R_g^3}{R^3} \tag{36}$$

Since our simulations will belong to the advective regime, basically We_2 will be used all the time. As it has been commented, the critical exponent has a different value depending on the situation. However, in all the calculations some symmetry arguments are supposed and this assumption cannot be considered any longer because the symmetry is broken with the attachment of the colloid. Therefore, the prescribed values of ν are not valid a priori in the advective regime and will be found later on. Considering the similarity principle, it is expected that if two different simulations behave equivalently, they should possess the same dimensionless group.

3 Results

Before entering deeply on the results analysis, let us show some results for a specific case just to familiarize the reader with the major output. Figures 4-7 display the time evolution of the intermonomeric distances (also including the distance between the first monomer and the base), the radius of gyration, the colloid velocity, and the velocity of the center of mass of the polymer for the following simulation parameters: $F = (0.0, 0.0, -0.1)$, $b = 0.1$, $N = 20$, $R_0 = 4.0b$, $k_bT = 2.13 \cdot 10^{-7}$, $k = 30.0 k_b T/b^2$, $\eta = 0.8$ for both fluid and

monomers, $R_c = 2.5 - 2.8$, and $dt = 0.01$. The notation of the colloid radius, R_c, includes first the real radius and then the effective hydrodynamic radius. All the simulations have been done in lattices periodic in the three directions. From now on, this set will be referred as the standard input parameters. For the standard parameters, $Pe \sim 1.3 \cdot 10^6$ and $A \sim 50$.

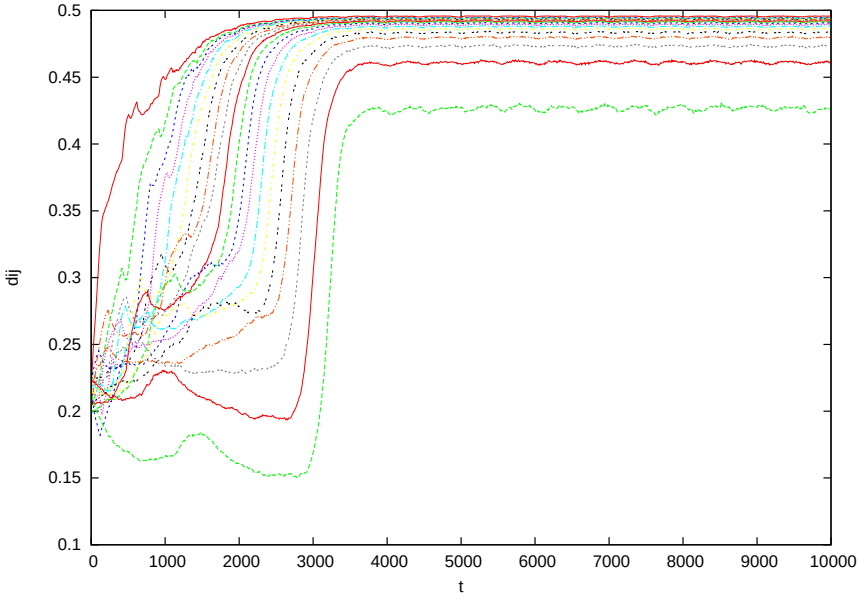

Figure 4: For the standard parameters, time evolution of the distances between monomers measured in lattice spacings and lattice time steps.

Taking a careful look to Figure 4, the fact that the distances tend to equilibrium in an orderly fashion is quite evident: first the distance between the base and the first bead increses gradually, meanwhile the subsequent beads follow the same tendency in a similar way. This behaviour can be explained with simple arguments: the colloid is advected because of the fluid forcing, thus starting to pull the first monomer and then the non-linear springs propagate the stretching until reaching the edge. When the polymer chain reaches a steady state, all the forces are balanced and the values of the distances decrease monotonocally from the base to the free end. In this state the colloid velocity and the velocity of the polymer center of mass are practically the same.

Of course, the radius of gyration is intimateley related with the inter-monomeric distances. Thus, this magnitude reaches also equilibrium at the same point as the distances do, i.e. when the distance between the last two monomers remains still ($t \sim 3500$ in Figures 4-5). Moreover, it seems that the smallest distances and the radius of gyration undergo some kind of oscillatations of period $\tau \sim 500$ in the steady state. Actually, this oscillation is present in all the distances, but its amplitude is greater near the polymer

tail.

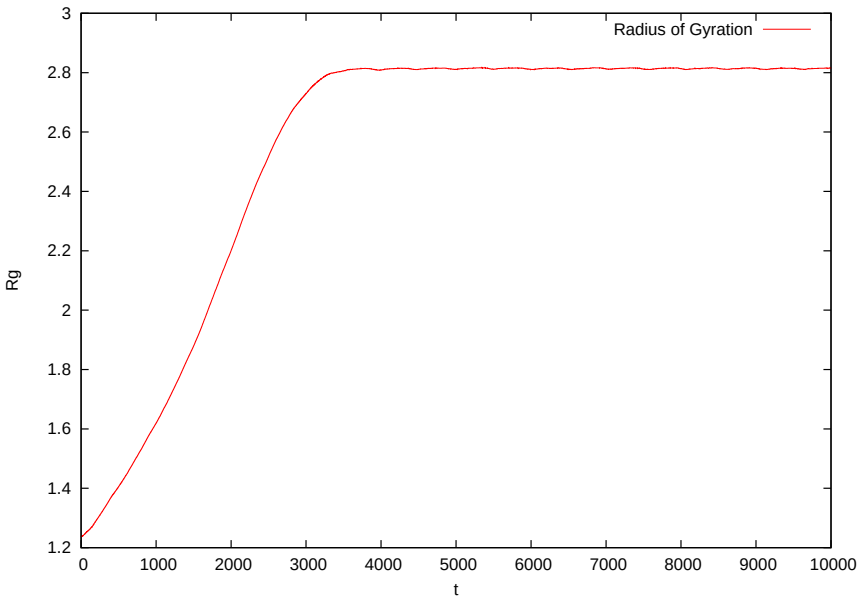

Figure 5: For the standard parameters, time evolution of the radius of gyration measured in lattice spacings and lattice time steps.

Figures 6 and 7 allows us to observe the so-mentioned oscillations more clearly. In both cases, it seems that a well-defined periodicity of $\tau \sim 500$ appears recurrently. In addition, since both objects possess the same velocity, it can be inferred that the polymer-colloid complex moves as a whole.

Let us talk about the velocities briefly. Obviously, the spanwise components of the velocities fluctuate in time, thus providing no net movement in the other coordinates. Concerning to the colloid case (Figure 6), firstly, the colloid moves as a bare colloid, but after some time its velocity begins to decrease until it reaches a new plateau corresponding to the stationary state. Due to the interaction between the polymer and the colloid, the new velocity is smaller in comparison with the bare colloid ($\sim 10\%$). The polymer is extended and exerts a significant force to the colloid, then reducing its velocity. This statement is in perfect agreement with what was expected because somehow the dimensions of the complex have increased substantually. About the polymer (Figure 7), in the first stages it has a random velocity (coming from the initialization process) that changes rapidly as the drag caused by the colloid becomes important. As the polymer stretches, it acquires the same velocity, as well as the same observed oscillations.

In order to unravel the nature of these oscillations and its effects on the polymer chain, some simulations varying one of the parameters at a time have been done. Among all the parameters, the most notorius variations occur when changing the forcing F, the viscosity η, and the colloid radius

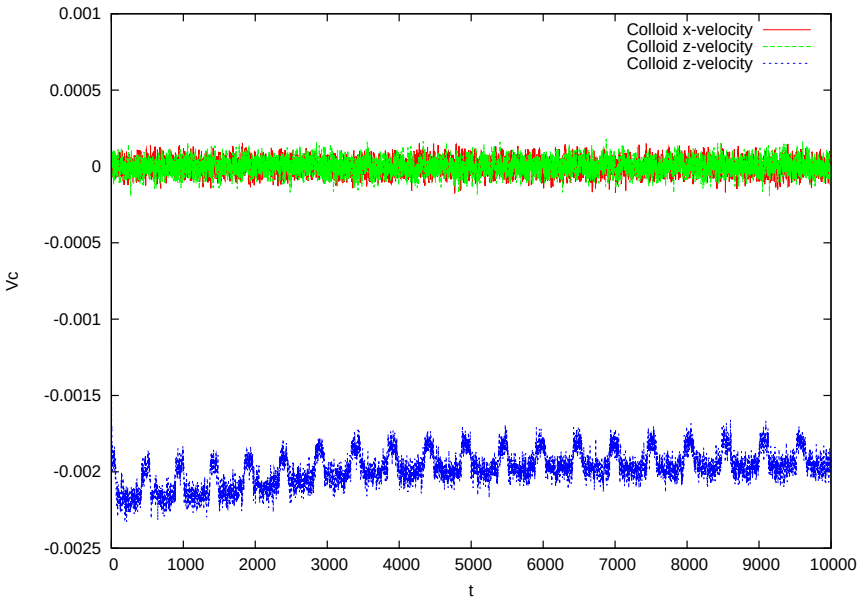

Figure 6: For the standard parameters, temporal evolution of the colloid velocity where the units of length and time are the lattice spacing and the lattice time steps.

R_c. Since all these parameters belong to the colloid, it can be suggested that the observed oscillations originate on the colloid and are transmitted to the chain when it is extended. In fact, the oscillations are always observable in the colloid velocity field (Figure 6), meanwhile they only appear on the polymer when it is elongated (Figure 7), in other words, when the coupling has manifested for sure. Moreover, the polymer configuration has been monitorized considering standard input parameters for approximately two periods (from $t \sim 4000$ to $t \sim 5000$) when it is elongated, and it seems that the chain is more oriented to the streamwise direction when the velocity is greater in modulus than when it reaches its maximum. This obervation could be related with the cyclic motion that a grafted polymer suffers under shear flow. In our case, the shear might be caused by the moving colloid and the polymer probably would suffer some periodic motion with some spatial reconfigurations. However, a deeper analysis should be done in that direction to correlate what has been expressed with the real situation. This feature represents another evidence of the coupling between them.

Let us now make some comments of a system with the standard parameters but without forcing, i. e. $Pe = A = 0$. The colloid and the center of mass of the polymer velocity fields fluctuate, yielding approximately zero for the mean velocity value. However, there seems to be a little advection for the colloid. In addition, the radius of gyration starts from a non-equilibrium conformation and decreases exponentially with a characteristic relaxation

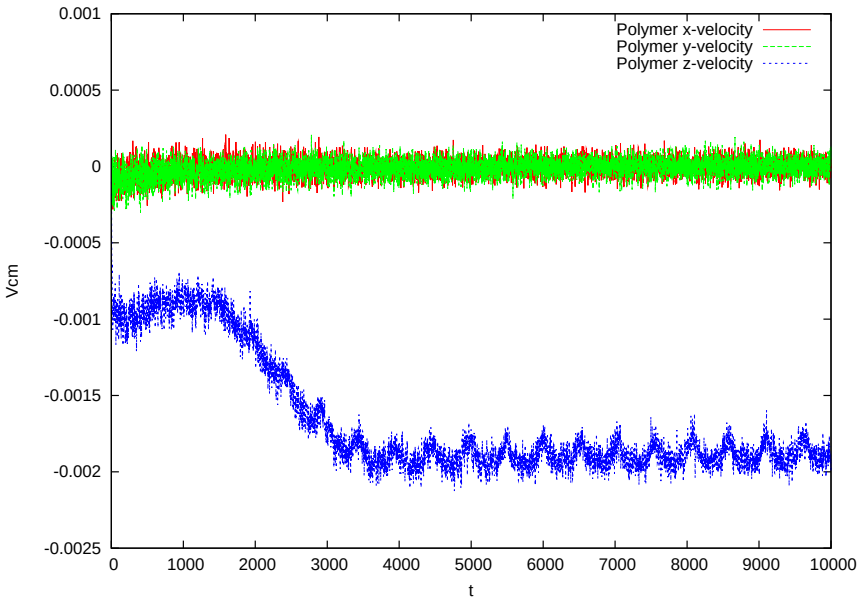

Figure 7: For the standard parameters, temporal evolution of the polymer centre of mass velocity where the units of length and time are the lattice spacing and the lattice time steps.

time. Curiously, in this case, the coil of the chain commences at the free tail and extends towards the colloid direction. This behaviour is completely the opposite of what happened in the case introduced in this section. The advection that the colloid has been experiencing is likely to be caused by the interaction with the first monomers because they possess a length greater than b and the relaxation process takes a long time to reach the other side. In the stationary state the polymer is coiled and both objects diffuse as free objects because the bind is extremely weak. The low Peclet regime has not been tackled exhaustiveley because the simulations need enormous amounts of time. However, by keeping $Pe \ll 1$ we are pretty sure that the dynamis are alike to the $Pe = 0$ case. An interesting question that could be studied in the future is the nature of the scaling of the radius of gyration in this regime and its similarity with the normal diffussion of a single polymer.

As we have already seen in the beginning of this section, the system dynamics in a high Peclet regime seems much richer. Figures 4-7 show the main features of a simulating frame with high advection ($A \sim 50$). At least, two more regions can be defined: moderate and low advection. For the moderate advective regime, the standard parameters are considered but with $F_z = -0.01$, so $Pe \sim 1.3 \cdot 10^5$ and $A \sim 5$. In this case, the results are analogous with the only difference that more time is necessary to arrive to the steady state and smaller extensions are obtained. Similarly, the low advective case imposes the standard parameters with $F_z = -0.001$, thus

resulting $Pe \sim 1.3 \cdot 10^4$ and $A \sim 0.5$. Somehow, this case is something between the low Peclet regime and the high-moderate trend. The monomer on the free tail tends to diffuse normally because no remarkable stresses are induced in the chain, meanwhile the nearest monomer to the colloid is being weakly advected. At some point the steady state is reached and both contributions balance. However, the polymer will be much less extended than in the other advective regimes.

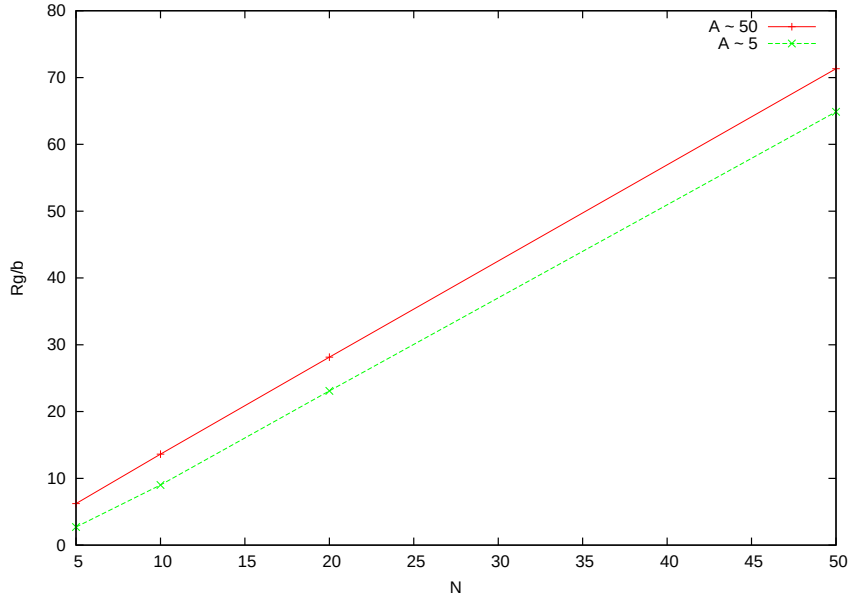

Figure 8: In a high Peclet regime, scaled radius of gyration as a function of N for $A \sim 50$ ($F_z = 0.1$) and $A \sim 5$ ($F_z = 0.01$) using the standard parameters.

Now, we want to make a more profound study of the high and moderate region because when the colloid is being advected notoriusly the polymer is stretched and the coupling manifests remarkably. Figures 8 and 9 show the dependance of the dimensionless radius of gyration and colloid steady velocity with the number of monomers. The normalizing factor V_0 is the steady velocity from simulations with the bare colloid. In all the simulations, the standard input parameters are taken with the only difference that $A \sim 50, 5$ correspond to $F_z = 0.1, 0.01$ respectively. From both plots, it is clear that the radius of gyration increases with the number of monomers, as well as the coupling between the colloid and the polymer becomes more important because the velocity is reduced drastically with the increase of N. Of course, when $A \sim 50$ the radius of gyration is greater than $A \sim 5$ because of the greater drag. Unexpectedly, both of them follow a clear linear tendency $R_g \propto N$ instead of a potential law $R_g \propto N^\nu$ with whom we are more used to. Then, the critical exponent might be considered one. Respectively,

the slopes for $A \sim 50, 5$ are $a \simeq 1.445 \pm 0.004, 1.387 \pm 0.009$, which are very similar. The trend for the stationary collloid velocities is not so evident. The one with the highest Peclet displays a linear trend meanwhile the other is not so clear. A plausible explanation of this not-so-intuitive behaviour could be provided by hydrodynamic reasons: for $A \sim 5$, the complex interacts more significantly with the surrounding fluid, so the viscosity affects more than when $A \sim 50$. Nevertheless, this question needs to be addressed more rigorously.

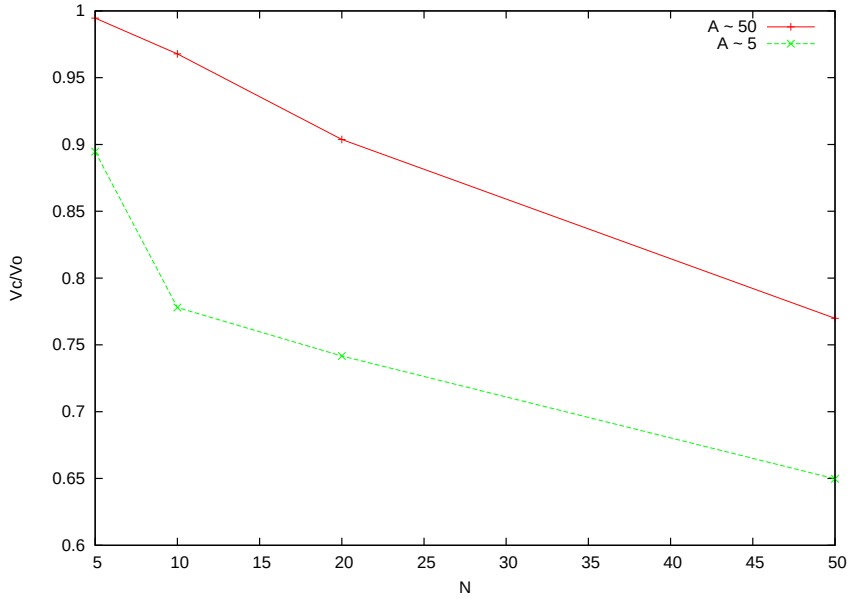

Figure 9: In a high Peclet regime, scaled colloid steady velocity as a function of N for $A \sim 50$ ($F_z = 0.1$) and $A \sim 5$ ($F_z = 0.01$) using the standard parameters.

A new question has been posed naturally because we have already seen that two systems with identical Pe and A are able to behave differently depending on the polymer parameters. To deal with this problem, the Weissenberg number comes into play. This number may help us to discern between the extensional regimes, but does not answer whether is the number of monomers or the the polymer length the important magnitude. Further simulations in this line have been done and some interesting results can be seen in Table 1.

The idea is to keep the total length approximately constant in an extended state for the polymer. In this state, most of the intermonomeric distances nearly take the maximum value $r_{\max} \simeq R_0 + b$. Two variations of the standard parameter values were considered where the product $r_{\max} N =$ constant: $b = 0.1$, $N = 50$ and $b = 0.25$, $N = 20$ for $A \sim 5, 50$. Contrasting the data for $A \sim 50$, the stationary radius of gyraton and the velocities

Pe	A	F_z	b	N	R_g/b	V_c/V_0	We
$\sim 1.3 \cdot 10^5$	~ 5	0.01	0.10	50	64.865	0.6608	$\sim 8.7 \cdot 10^4$
$\sim 1.3 \cdot 10^5$	~ 5	0.01	0.25	20	68.973	0.7428	$\sim 1.0 \cdot 10^5$
$\sim 1.3 \cdot 10^6$	~ 50	0.1	0.10	50	71.323	0.7699	$\sim 1.2 \cdot 10^6$
$\sim 1.3 \cdot 10^6$	~ 50	0.1	0.25	20	71.750	0.7676	$\sim 1.2 \cdot 10^6$

Table 1: Some results based on variations of the polymer parameters, where V_0 is the colloid steady velocity considering simulations with the bare colloid. The remaining parameters are the standard ones. The Weissenberg number is computed using the obtained R_g.

are much more alike than for $A \sim 5$. In fact for $A \sim 50$, $\sim 0.6\%$ for the radius of gyration and $\sim 0.3\%$ for the steady velocities. As a consequence, considering the fact that both situations have the same properties the dimensionless group that governs the system ought to be almost the same. For the other case ($A \sim 50$), the radius of gyration and the steady velocities differ approximately in a $\sim 6\%$ and $\sim 12\%$, respectiveley. In any case, the critical exponent of the Weissenberg number should be $\nu \simeq 1$ and $R_g \sim bN$ with a proportionality factor that may depend on each case. Therefore, the Weissenberg number is computed with the radius of gyrations obtained from the calculations.

In the advective regime, the Weissenberg number represents the ratio between the time that the polymer needs to move a radius length versus the necessary time for the polymer to relax. Hence, in the low We cases, the polymer has more time to interact with the fluid as it does for higher Weissenberg numbers. In the same way as before, some hydrodynamic interactions may be more relevant at low We that can enhance the velocity reduction and explain our observations. Nevertheless, whether this hypothesis is valid or not to explain the large variations observed in the two cases with $A \sim 5$ is not so clear and should be tackled in future studies.

4 Conclusions

There is no doubt that our model couples the colloid and the polymer. On the one hand, the polymer slowed down its velocity when the polymer began the stretching. On the other hand, the polymer increases its size due to the colloid drag, thus acquiring its steady velocity and their properties, such as the so-mentioned oscillations.

Even though more accurate measurements are desirable for the observed oscillations, it looks like they may be created in the colloid and then transferred to the polymer. In analogy with the case of a grafted polymer under shear flow, all the necessary ingredients are present (a shear rate characteristic of the flow and a polymer attached to a surface), so the system is a

promising candidate to show similar features.

The symmetry breaking of the polymer chain is really a noteworthy fact. Some preliminar calculations were carried out only with the polymer in different confinements and forcings. When the polymer diffuses freely or in a in a channel, the intermonomeric distances are the same in statistical terms. When the polymers stretches due to some kind of forcing, the distances adopt a symmetric trend respect to the middle point. All this characteristics disappear when the colloid is included because the nearest monomer is the most stretched, whilst the furthest is the least one. The search of the critical exponents in the high and moderate advective regime has determined that $\nu \simeq 1$. Even at low Peclet numbers and low advective regimes, the diffusion is not the usual. However, it would be of great interest to determine how the criticality of the chain changes in the different regions and if possible, determine $\nu(Pe, A, We)$.

About the results, it would be desirable to carry out more simulations and try to characterize the advective and diffusive region more exhaustively and determine completely how the radius of gyration and the steady velocities depend on Pe, A, and We, as well as which is their exact role. From our brief study it seems that the the total length is the most relevant parameter in the polymer because by keeping this magnitude almost constant, very similar results are recovered. It might be interesting to see the regions where this premise is valid and how it might change.

Also, in order to get a better approach to the real system and avoid possible finit-size effects, exploring the whole parameter space with systems of greater dimensions would be of great asset, i.e. increasing the lattice size, the colloid and the polymer size. Moreover, the same model could be used to study other effects that shall be only present in confined geometries under different kinds of forcing (Couette or Poisseuille) or colloids with more than one polymer attached to it. Last but not least, further studies could try to improve the simulation employing a more realistic biopolymer, like a worm-like chain (WLC) model, and then try to compare with real observations.

References

[1] F. Ritort, *Single-molecule experiments in biological physics: methods and applications*, J. Phys.: Condens. Matter **18**, 531-583 (2006)

[2] L. E. Reichl, *A Modern Course on Statistical Physics*, (Wiley and Sons, 1998)

[3] J. F. Marko and E. D. Siggia, *Stretching DNA*, Macromolecules **28**, 8759 (1995)

[4] R. Delgado-Buscaloni, *Cyclic motion of a Grafted Polymer Under Shear Flow*, Phys. Rev. Lett. **96**, 088303 (2006)

[5] M. Doi, *Introduction to Polymer Physics*, (Oxford University Press, 1996)

[6] M. Doi and S. F. Edwards, *The Theory of Polymer Physics*, (Oxford University Press, 1994)

[7] A. Taroni, *New route to polymer-protein hybrid materials*, Materials Today **11** (2008)

[8] P. C. Nelson, *Biological Physics*, (W. H. Freeman, 2004)

[9] S. Succi, *The Lattice Boltzmann Equation for Fluid Dynamics and Beyond*, (Oxford University Press, 2001)

[10] Haiping Fang *et al*, *Lattice Boltzmann method for simulating the viscous flow in large distensible blood vessels*, Phys. Rev. E **65**, 051925 (2002)

[11] R. M. H. Merks *et al*, *Problem-Solving Environments for Biological Morphogenesis* , Computational Biology **65**, 61-72 (2006)

[12] A. J. C. Ladd and R. Verberg, *Lattice-Boltzmann Simulations of Particle-Fluid Suspensions*, J. Stat. Phys. **104**, 1191-1251 (2001)

[13] B. Dunweg A. J. C. Ladd, *Lattice Boltzmann Simulations of Soft Matter Systems*, Adv. Comp. Sim. Appr. for Soft Matter Sc. III **221** (2009)

[14] P. Ahlrichs and B. Dunweg, *Lattice Boltzmann simulation of polymer-solvent systems*, Int. J. Mod. Phys. C **9**(8), 1429 (1998)

[15] P. Ahlrichs and B. Dunweg, *Simulation of a single polymer chain in solution by combining Lattice Boltzmann and molecular Dynamics*, J. Chem. Phys. **111**, 8225 (2005)

[16] O. B. Usta *et al*, *Lattice-Bolttzmann simulations of the dynamics of polymer solutions in periodic and confined geometries*, J. Chem. Phys. **122**, 094902 (2005)

[17] L. D. Landau and E. M. Lifshitz, *Fluid Mechanics*, (Pergamon Press, 1993)

[18] M. P. Allen and D. J. Tildesley, *Computer Simulation of Liquids*, (Oxford University Press, 1987)

[19] J. M. Haile, *Molecular Dynamics Simulation: Elementary Methods*, (John Wiley and Sons, 1992)

[20] E. Guyon *et al*, *Physical Hydrodynamics*, (Oxford University Press, 2001)

[21] R. G. Larson, *The Structure and Rheology of Complex Fluids*, (Oxford University Press, 1999)